

# We are IntechOpen, the world's leading publisher of Open Access books Built by scientists, for scientists

6,900

Open access books available

186,000

International authors and editors

200M

Downloads

Our authors are among the

154

Countries delivered to

TOP 1%

most cited scientists

12.2%

Contributors from top 500 universities



WEB OF SCIENCE™

Selection of our books indexed in the Book Citation Index  
in Web of Science™ Core Collection (BKCI)

Interested in publishing with us?  
Contact [book.department@intechopen.com](mailto:book.department@intechopen.com)

Numbers displayed above are based on latest data collected.  
For more information visit [www.intechopen.com](http://www.intechopen.com)



# Biorthogonal Decomposition for Wide-Area Wave Motion Monitoring Using Statistical Models

P. Esquivel<sup>1</sup>, D. Cabuto<sup>1</sup>, V. Sanchez<sup>2</sup> and F. Chan<sup>2</sup>

<sup>1</sup>*Technological Institute of Tepic, Electrical and Electronics Engineering Division, Nayarit,*

<sup>2</sup>*University of Quintana Roo, Sciences and Engineering Division, Quintana Roo*

*México*

## 1. Introduction

Characterization of spatial and temporal changes in the dynamic pattern that arise when a wide-area system is subjected to a perturbation becomes a significant problem of great theoretical and practical importance. The computation time required to solve large analytical models might become prohibitive for practical systems. Thus, to reduce the complexity of the problem, several simplifications have been commonly used which may result in a poor characterization of global system behaviour. Therefore, a great deal of attention has been paid to identify and to characterize oscillatory activity in large interconnected systems through use of wide-area monitoring schemes such as global positioning systems (GPS) based in multiple phasor measurements units (PMUs) (Messina, et al., 2010). When simultaneously measured responses throughout an interconnected system are available, modal behaviour should be extracted using correlation techniques rather than individual analysis of the system response. This provides a global picture on the system behaviour and enables statistical characterization of the observed phenomena. The problem of selecting the most significant modes is of considerable interest and it has been studied intensively for several researchers (Esquivel & Messina, 2008; Hannachi, et al., 2007; Hasselmann, 1988; Holmes, et al., 1996; Kwasniok, 1996, 2007). Statistical models have been widely used in many engineering and science applications for the analysis of space-time varying system response from measured data (Aubry, et al., 1990; Dankowicz, et al., 1996; Delsole, 2001; Lezama et al., 2009; Messina, et al., 2010, 2011; Spletzer, et al., 2010); i.e., unsteady fluid flow (Terradas, et al., 2004), turbulence (Hannachi, et al. 2007; Leonardi, et al., 2002; Susanto, et al., 1997; Toh, 1987), optimal control (Wallaschek, 1988), structural dynamics (Feeny & Kappagantu, 1998; Han & Feeny, 2003; Holmes, et al., 1996; Marrifield & Guza, 1990; Oey, 2007), heat transfer (Barnett, 1983; Kaihatu, et al., 1997) and system identification have been reported (Esquivel, et al., 2009; Feeny, 2008; Hasselmann, 1988; Horel, 1984; Kwasniok, 1996, 2007). These methodologies use statistical techniques such as, empirical orthogonal function (EOF) (Esquivel & Messina, 2008), principal interaction pattern (PIP) (Achatz, et al., 1995), principal oscillation pattern (POP) (Hasselmann, 1988),

optimal persistent pattern (OPP) (DelSol, 2001), and the canonical correlation analysis (CCA) (Kwasniok, 2007) that capture various forms of spatio-temporal variability. Among other approaches, empirical orthogonal functions (EOFs) have been used since the mid-1970s for the identification of space-time dynamic systems. More recently, these techniques have gained wide popularity in applications related to wide-area data analysis and reduced-order modelling of various physical processes or models (Messina, et al. 2010; Spletzer, et al., 2010). Underlying issues of these techniques, such as the estimation and localization of propagating and standing features that may be associated with observed or measured data and their applications to space-time varying processes do not seem to be recognized or, at least, they have not been reported. This fact motivates the derivation of a model based on statistical techniques to identify the behaviour of multivariate processes such as the seismic wave propagation components that surge during an earthquake which involve variability over both space and time. These processes may contain moving patterns, travelling waves of different spatial scales and temporal frequencies that are proposed to identify in our study using complex EOF analysis.

## 2. Theoretical fundamentals of empirical orthogonal functions

The conventional analysis of empirical orthogonal functions is primarily a method of compressing of time and space variability of a data set into the lower possible number of spatial patterns. Each one of these patterns is composed of standing modes of variability and modulated by a time function. The conventional formulation of EOF analysis involves a set of optimal basis which is forced to approach the original field with modes at infinite frequency. In this section is shown that this requirement reduces the ability in the conventional method to characterize the travelling and standing features in dynamical systems because the spatial variation of the original field are combined with the temporal variations. As such, conventional-EOF analysis detects only standing wave components, not travelling wave components. The key point to observe is that real-EOF analysis cannot deal with propagating features and it only uses spatial correlation of the data set, it is necessary to use both spatial and time information in order to identify such features (Esquivel, 2009). In this chapter, we extend the conventional empirical orthogonal function analysis to the study and detection of propagating features in nonlinear patterns such as seismic wave propagation components that surge during an earthquake recorded from wide-area monitoring schemes such as GPS-based in multiple PMUs, most of the notation used in this text is standard, vectorial quantities are denoted by boldface letters and scalar quantities by italic letters; others symbols used in the text are too defined. Unlike the real case, complex EOF analysis allows compressing the data into the lowest possible number of spatial patterns, each one composed of modes of variability, which may be either travelling or standing modes. The technique allows us to explicitly describe and localize standing and propagating oscillations to the leading seismic wave as a number of complex empirical modes.

In this section, we provide a spatio-temporal decomposition based in the use of time synchronized measured data recorded from multiple phasor measurement units (PMUs) in dynamical systems to cope with increasing complexity of information in the use of wide-area monitoring schemes. The methodology is proposed to identify and extract dynamically independent spatio-temporal patterns using a biorthogonal decomposition based in the complex EOF analysis and the separability of complex correlation functions

considered from a statistical perspective (Aubry, et al., 1990; Dankowicz, et al., 1996; Spletzer, et al., 2010). This approach provides an efficient and accurate way to compute standing and propagating features of general nonstationary processes identifying important information for the analysis of dynamical phenomena such as seismic wave components recorded from earthquakes. Moreover, this may lead to greater understanding of the oscillatory activity in interconnected systems. The method allows the introduction of several measures that define moving features in space-time varying fields as: spatial amplitude and phase function, temporal amplitude and phase function, spatial and temporal energy, wave number, angular frequency and average phase speed (Barnett, 1983; Esquivel & Messina, 2008; Susanto, et al. 1997; Terradas, et al., 2004; Hannachi, et al., 2007). The method developed is general and could be applied without loss of generality to measured or simulated data. As an illustrative case, the method is applied to a synthetic example; additionally, data recorded from GPS-based multiple phasor measurements units from a real event of seismic wave components recorded during a submarine earthquake are used to study the practical applicability of the method to characterize spatio-temporal behaviour in wide-area systems.

## 2.1 Theoretical development

Empirical orthogonal function (EOF) analysis is a procedure for extracting a basis for a modal decomposition from an ensemble of signals in multidimensional measurements. A very appealing property of the basis is its optimality. Among all possible decompositions of a random field, the EOF analysis is the most efficient in the sense that for a given number of modes, the projection on the subspace used for modelling the random field will on average contain the most energy possible. Although EOF analysis has been regularly applied to non-linear problems (Marrifield & Guza, 1990; Susanto, et al., 1997; Toh, 1987; Kaihatu, et al., 1997), it is essential to underline that it is a linear technique and that it is optimal only with respect to other linear representations. Empirical orthogonal function analysis, also known as proper orthogonal decomposition (POD) and Karhunen-Loève transform was introduced by (Kosambi, 1943). It is also worth pointing out that EOF analysis is closely related to principal component analysis (PCA) introduced by (Hotelling, 1933). For a detailed historical review of POD or PCA, the reader is referred to (Barnett, 1983; Hasselmann, 1988; Hostelling, 1933; Horel, 1984; Kosambi, 1943; Toh, 1987).

Let

$$u(x,t) \quad (1)$$

be a zero mean random field on a domain  $\Omega$ . In practice, the field is sampled at a finite number of points in time. Then, at time  $t_k$ , the system displays a snapshot  $u(x,t_k)$  which is a continuous function of  $x$  in  $\Omega$ . The aim of the EOF analysis is to find the most persistent structure among the ensemble of  $N$  snapshots. More precisely, assume that  $\mathbf{X}(x_j,t_k)$ ,  $j=1,\dots,n$  and  $k=1,\dots,N$  denotes a sequence of observations on some domain  $x \in \Omega$  where  $x$  is a vector of spatial variables, and  $t_k$  is the time at which the observations are made. The method of EOF analysis, both spatial and time-dependent, is a specification of the general theory of expansion of random functions (random fields or random processes) in a series of some deterministic (nonrandom) functions with random uncorrelated coefficients (Feeny & Kappagantu, 1998). The essential idea of the proper orthogonal decomposition is to generate

an optimal basis,  $\varphi(x)$ , for the representation of an ensemble of data collected from measurements or numerical simulations of a dynamic system as is shown in Fig. 1.

Given an ensemble of measured data, the data set can be written as the  $N \times n$ -dimension matrix

$$\mathbf{X}(x_j, t_k) = \begin{bmatrix} u(x_1, t_1) & \cdots & u(x_n, t_1) \\ \vdots & \ddots & \vdots \\ u(x_1, t_N) & \cdots & u(x_n, t_N) \end{bmatrix} \quad (2)$$

where typically  $n \neq N$ , so  $\mathbf{X}$  is generally rectangular (Messina, et al., 2010). The technique yields an orthogonal basis for linear, infinite-dimensional Hilbert space  $L^2([0,1])$ , that maximizes the averaged projection of the response matrix for the representation of the ensemble of data that is fully orthogonal, and it is assumed to be normalized, i.e.,

$$\max_{\varphi_j(x) \in L^2([0,1])} \frac{\langle |\langle \mathbf{X}(x, t), \varphi_j(x) \rangle|^2 \rangle}{\|\varphi_j(x)\|^2} \quad \text{subject to} \quad \|\varphi_j(x)\|^2 = 1 \quad (3)$$

where  $|\cdot|$  denotes the modulus,  $\|\cdot\|$  is the  $L^2$ -norm and,  $\langle \cdot \rangle$  implies the use of an average operation (Holmes, et al., 1996). The corresponding functional for the constrained variational problem is solved and reduced to:

$$\int_0^1 \left[ \int_0^1 \langle \mathbf{u}(x) \mathbf{u}^*(x') \rangle \varphi(x') dx' - \lambda \varphi(x) \right]^* \psi^*(x) dx = 0 \quad (4)$$

where the  $(*)$  denotes the conjugate transpose (sometimes denoted as Hermitian,  $H$ ), and the  $(\cdot)$  denotes transpose vector. Thus, if  $\psi^*(x) = 0$ , the optimal basis are given by the eigenfunctions  $\varphi_j(x)$  of the integral equation,

$$\int_0^1 \langle \mathbf{u}(x) \mathbf{u}^*(x') \rangle \varphi(x') dx' = \lambda \varphi(x) \quad (5)$$

whose kernel is the averaged autocorrelation function  $\langle \mathbf{u}(x) \mathbf{u}^*(x') \rangle \triangleq \mathbf{C}(x, x')$ . Under this assumption, the integral (5) can be written as

$$\mathbf{C} \varphi(x) = \lambda \varphi(x) \quad (6)$$

where the resulting autocorrelation matrix  $\mathbf{C}$ , is real, symmetric, positive and semi-definite matrix. Therefore, the optimization problem can be recast as the problem of finding the largest eigenvectors,  $\varphi(x)$ , of the equation (6), called empirical orthogonal functions (EOFs); its corresponding eigenvalues are real, nonnegative, and ordered so that  $\lambda_1 \geq \lambda_2 \geq \dots \geq \lambda_j \geq 0$ . This method, also called conventional EOF analysis, cannot be used to detect propagation features due to the assumption that each field is represented as a spatial fixed pattern of behaviour and lack of phase information, becoming prohibitive to practical applications.

Now, if we assume that  $\psi^*(x) \neq 0$ , then (4) can be rewritten as

$$\int_0^1 \int_0^1 \varphi^*(x') \langle u(x) u^*(x') \rangle \psi^*(x) dx' dx = \int_0^1 \varphi^*(x) \lambda \psi^*(x) dx \quad (7)$$

such that, the inner product  $(\varphi^*(x) C \psi^*(x)) \neq 0$ , with orthogonal eigenvectors  $\varphi(x)$ ,  $\psi(x)$ , i.e.,

$$\varphi_i^T \varphi_j = \begin{cases} 0, & i \neq j \\ \delta(\varphi), & i = j \end{cases} \text{ and } \psi_i^T \psi_j = \begin{cases} 0, & i \neq j \\ \delta(\psi), & i = j \end{cases} \quad (8)$$

From (4) it can be seen that if there exists an arbitrary variation (spatial),  $\psi^*(x) \neq 0$ , then the original field can be reconstructed using two optimal orthogonal basis given from (7). Based in this notion, an efficient technique to find the optimal basis using complex EOF analysis (CEOFs) is proposed (Esquivel, 2009).

Our proposed methodology based in EOF analysis and the Hilbert transform is developed to be applied for representations of complex data fields in a biorthogonal decomposition illustrating the phenomenon of spatial and temporal variability in interconnected systems. This method consists first in extend each real field data to the complex world using the Hilbert transform to provide the phase information; and second, the EOF analysis is developed to the complex data field for the detection and localization of propagation features into dynamical systems.

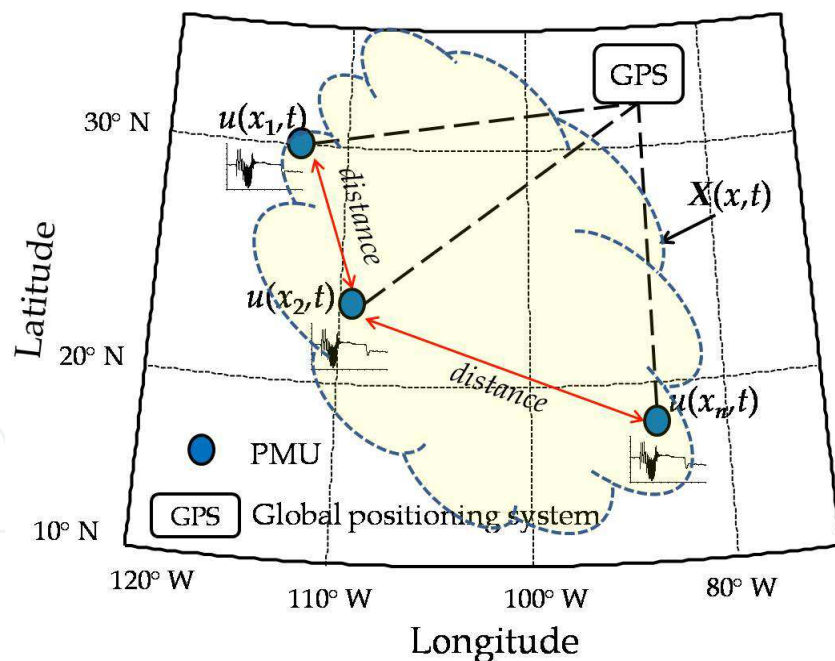


Fig. 1. Global positioning system (GPS) and PMU data in terms of a time-space varying field.

## 2.2 Complex data fields

Conventional EOF analysis of real-data fields is commonly carried out under the assumption that each field can be represented as a spatially fixed pattern of behaviour. This method, however, cannot be used for detection of propagating features because of the lack

of phase information (Esquivel & Messina, 2008). To fully utilize the data, a technique is necessary unknowing the nonstationarity of the time-series data.

Let  $u(x_j, t_k)$  be a space-time varying scalar field representing a time series recorded from a wide-area distribution system, where  $x_j, j=1, \dots, n$  is a set of spatial variables on a space  $\Omega$ , and  $t_k, k=1, \dots, N$  is the time at which the observations are made. Provide  $u(x, t)$  is simple and square integrable, it has a Fourier representation of the form

$$u(x_j, t) = \sum_{m=1}^{\infty} [a_{j(m)}(\omega) \cos(m\omega t) + b_{j(m)}(\omega) \sin(m\omega t)] \quad (9)$$

where  $a_{j(m)}(\omega)$  and  $b_{j(m)}(\omega)$  are the Fourier coefficients defined as

$$a_{j(m)} = \frac{1}{\pi} \int_{-\pi}^{\pi} u(x_j, t) \cos(m\omega t) d\omega$$

$$b_{j(m)} = \frac{1}{\pi} \int_{-\pi}^{\pi} u(x_j, t) \sin(m\omega t) d\omega \quad (10)$$

This allows the description of travelling waves propagating throughout the system. Equation (9) can be rewritten in the form

$$u_c(x_j, t) = \sum_{m=1}^{\infty} c_{j(m)}(\omega) e^{-im\omega t} \quad (11)$$

where  $c_{j(m)}(\omega) = a_{j(m)}(\omega) + ib_{j(m)}(\omega)$ ,  $i = \sqrt{-1}$  is the unit complex number. Expanding (11) and collecting terms gives

$$u_c(x_j, t) = \sum_{m=1}^{\infty} \{ [a_{j(m)}(\omega) \cos(m\omega t) + b_{j(m)}(\omega) \sin(m\omega t)] \}$$

$$+ i \sum_{m=1}^{\infty} \{ [b_{j(m)}(\omega) \cos(m\omega t) - a_{j(m)}(\omega) \sin(m\omega t)] \} \quad (12)$$

$$= u(x_j, t) + i u_H(x_j, t)$$

where the real part of  $u_c(x_j, t)$  is given by (9) and the imaginary part is the Hilbert transform of  $u(x_j, t)$ . In formal terms, the Hilbert transform of a continuous time series  $u(x_j, t)$  is defined by the convolution

$$u_H(x_j, t) = \frac{1}{\pi} \int_{-\infty}^{\infty} \frac{u(y)}{t-y} dy \quad (13)$$

where the integral is taken to mean the Cauchy principal value. The most well-known classical methods for computing the Hilbert transform are derived from the Fourier transform. However, this transform has a global character and hence, it is not suitable for the characterization of local signal parameters. Alternatives for local implementation of the Hilbert transformation which are based on local properties are developed and tested in this analysis (Hannchi, et al., 2007; Lezama, et al., 2009; Terradas, et al., 2004; Barnett, 1983).

For discretely sampled data, the Hilbert transform can be derived in the time domain by applying a rectangular rule to (13). It can be shown that

$$u_H(x_j, t) \approx \frac{2}{\pi} \sum_{k=-\infty}^{\infty} \frac{u(t + (2k + 1)\tau)}{2k + 1} \quad (14)$$

where  $\tau$  is the step size. When (13) is applied to a discrete time series  $u(x_j, t)$ ,  $k=0, \pm 1, \dots$ , we get

$$\begin{aligned} u_H(x_j, t_k) &= \frac{2}{\pi} \sum_{k=-\infty}^{\infty} \frac{u(t + 2k + 1)}{2k + 1} \\ &= \frac{2}{\pi} \sum_{k \geq 0} \frac{1}{2k + 1} [u(t + 2k + 1) - u(t - 2k - 1)] \end{aligned} \quad (15)$$

In previous formulations, the Hilbert transform was estimated by truncating the series (15). This truncation was approximated using a convolution filter as

$$u_H(x_j, t_k) = \sum_{\ell=-L}^L u(x_j, t_k - \ell) h(\ell), \quad L = \infty \quad (16)$$

where  $h$  is a convolution filter with an unit amplitude response and  $90^\circ$  phase shift. In this research, it has been found that a simple filter that has the desired properties of approximate unit amplitude response and  $\pi/2$  phase shift is given by

$$h(l) = \begin{cases} \frac{2}{\pi l} \sin^2(\pi l/2), & l \neq 0 \\ 0, & l = 0 \end{cases} \quad (17)$$

where  $-L \leq l \leq L$ . We omit the calculations.

As  $L \rightarrow \infty$ , equation (16) yields an exact Hilbert transform. This represents a filtering operation upon  $u(x_j, t)$  in which the amplitude of each Fourier spectral component remains unchanged while its phase is advantaged by  $\pi/2$ . In (Hannachi, et al., 2007) has been found that  $7 \leq L \leq 25$  provides adequate values for the filter response.

In what follows, we discuss the extension of the conventional EOF analysis using the above approach to compute standing and propagating features of general nonstationary processes where the eigenvectors of the covariance matrix are complex and it can be expressed alternatively as a magnitude and phase pair.

### 3. Complex empirical orthogonal function analysis

The method of complex EOF analysis is an optimal technique of biorthogonal decomposition to find a spatial and temporal basis that spans an ensemble of data collected from experiments or numerical simulations. The method essentially decomposes a fluctuating field into a weighted linear sum of spatial orthogonal modes and temporal orthogonal modes such that the projection onto the first few modes is optimal.

Drawing on the above approach, an efficient formulation to compute a complex expansion for the data set has been derived.

Assume that  $\mathbf{X}(x,t)$  is augmented by their imaginary components to form a complex data matrix such as (Esquivel, 2009)

$$\mathbf{X}_c(x,t) = \mathbf{X}_R(x,t) + i\mathbf{X}_I(x,t) \quad (18)$$

where the subscripts  $c$ ,  $R$  and  $I$  indicate the complex, real and imaginary vectors respectively. Implicit in the model is the assumption that  $\mathbf{X}_c$  can be represented as

$$\mathbf{X}_c = \|\mathbf{X}_c\| [\cos(\boldsymbol{\theta}_{X_c} t) + i\sin(\boldsymbol{\theta}_{X_c} t)] \quad (19)$$

where  $\|\mathbf{X}_c\|$  and  $\boldsymbol{\theta}_{X_c}$  are the magnitude and phase of  $\mathbf{X}_c$ . Under this assumption, the complex autocorrelation matrix becomes,

$$\mathbf{C} = \frac{1}{N} \mathbf{X}_c^H \mathbf{X}_c \quad (20)$$

where it is straightforward to show that the autocorrelation matrix  $\mathbf{C}$ , for the case complex data can be written in the form  $\mathbf{C} = \mathbf{C}_R + i\mathbf{C}_I$  which the real part is a symmetrical matrix, (i.e.,  $\mathbf{C}_R = \mathbf{C}_R^T$ ) and the imaginary part is a skew-symmetric matrix (i.e.,  $\mathbf{C}_I^T = -\mathbf{C}_I$ ). If the size of  $\mathbf{C}_I$  is odd, then the determinant of  $\mathbf{C}_I$  will always be zero. Because the symmetrical matrix is a particular case of the Hermitian matrix, then all its eigenvectors are real. Furthermore, the eigenvalues of the skew-symmetric matrix are all imaginary pure and, it is a normal matrix; its eigenvectors are complex conjugate.

From (20), It can be easily verified that

$$\begin{aligned} \mathbf{X}_c^H \mathbf{X}_c &= \|\mathbf{X}_c^T\| \|\mathbf{X}_c\| [\cos(\boldsymbol{\theta}_{X_c^T} t) - i\sin(\boldsymbol{\theta}_{X_c^T} t)] [\cos(\boldsymbol{\theta}_{X_c} t) + i\sin(\boldsymbol{\theta}_{X_c} t)] \\ &= \|\mathbf{X}_c^T\| \|\mathbf{X}_c\| \{ [\cos(\boldsymbol{\theta}_{X_c^T} t)\cos(\boldsymbol{\theta}_{X_c} t) + \sin(\boldsymbol{\theta}_{X_c^T} t)\sin(\boldsymbol{\theta}_{X_c} t)] \\ &\quad + i[\cos(\boldsymbol{\theta}_{X_c^T} t)\sin(\boldsymbol{\theta}_{X_c} t) - \sin(\boldsymbol{\theta}_{X_c^T} t)\cos(\boldsymbol{\theta}_{X_c} t)] \} \end{aligned} \quad (21)$$

From the decomposition given in (21) can be seen that the imaginary part is zero when the time is in phase with the extremum of the cosine or sine, that is, the sum of the two components is zero; at this time instant both are symmetrical matrices (Feeny, 2008). The imaginary part of (21) measures the degree of asymmetry when the sum of both matrices is different from zero; this is used to define the existence of arbitrary variations into the space,  $\boldsymbol{\Psi}^*(x) \neq 0$ ; this feature is used to define the existence of travelling wave components in the space-time varying fields and to determine leading seismic wave propagation components.

From the decomposition for the complex autocorrelation matrix (20), the optimal basis for the proposed spatio-temporal decomposition is defined by the eigenfunctions  $\boldsymbol{\phi}_R(x)$  and  $\boldsymbol{\phi}_I(x)$  for the real and imaginary part respectively. A test to split the spatial-temporal covariance functions is given by (Wallaschek, 1988; Fuentes, 2006).

Once the spatial eigenvectors associated with real and imaginary part of (20) are computed, the original field can be approximated by a spatio-temporal model. Assuming that this model is composed of standing and travelling wave components, the space-time varying field can be written as

$$\mathbf{X}(x, t) = \mathbf{X}_{swc}(x, t) + \mathbf{X}_{twc}(x, t) \quad (22)$$

where  $\mathbf{X}_{swc}$  and  $\mathbf{X}_{twc}$  denotes the standing and travelling wave components respectively. Therefore, the associated approximation for the complex data field (19) in terms of a truncated sum of dominant modes (EOFs basis)  $p$  and  $q$ , is defined as

$$\mathbf{X}_c(x, t) = \sum_{j=1}^p \mathbf{A}_{R(j)}(t) \boldsymbol{\Phi}_{R(j)}^H(x) + i \sum_{j=1}^q \mathbf{A}_{I(j)}(t) \boldsymbol{\Phi}_{I(j)}^H(x) \quad (23)$$

where the time-dependent complex coefficients associated with each eigenfunction,  $\mathbf{A}_{R(j)}(t)$  and  $\mathbf{A}_{I(j)}(t)$  are obtained as the projection of the basis  $\boldsymbol{\Phi}_{R(j)}(x)$  and  $\boldsymbol{\Phi}_{I(j)}(x)$  respectively into complex field  $\mathbf{X}_c$  of the form

$$\begin{aligned} \mathbf{A}_{R(j)}(t) &= \mathbf{X}_c \boldsymbol{\Phi}_{R(j)}(x) \\ \mathbf{A}_{I(j)}(t) &= \mathbf{X}_c \boldsymbol{\Phi}_{I(j)}(x) \end{aligned} \quad (24)$$

These complex coefficients are conveniently split into their amplitude and phase, therefore, from the complex model (23), the ensemble of data can be expressed as

$$\mathbf{X}_c(x, t) = \sum_{j=1}^p \mathbf{R}_{R(j)}(t) \mathbf{S}_{R(j)}(x) e^{i(\boldsymbol{\theta}_{R(j)}(t) + \boldsymbol{\Phi}_{R(j)}(x))} + \sum_{j=1}^q \mathbf{R}_{I(j)}(t) \mathbf{S}_{I(j)}(x) e^{i(\boldsymbol{\theta}_{I(j)}(t) + \boldsymbol{\Phi}_{I(j)}(x) + \pi)} \quad (25)$$

where  $\mathbf{R}(t)$  and  $\mathbf{S}(x)$  are the temporal and spatial amplitude functions associated with the wave decomposition respectively and,  $\boldsymbol{\theta}(t)$  and  $\boldsymbol{\Phi}(x)$  are the temporal and spatial phase function.

Now, four measurements that define moving features in  $\mathbf{u}(x, t)$  can then be defined:

1. Spatial distribution of variability of each eigenmode
2. Relative phase fluctuation
3. Temporal variability in magnitude
4. Variability of the phase of a particular oscillation

The succeeding sections describe the properties of these representations to assess and to extract swing oscillations patterns and modal characteristics directly from recorded data in wide-area dynamical systems. It is shown that the proposed method can be used to predict the correct spatial location in the modal distribution of seismic wave.

### 3.1 Spatial amplitude function, $\mathbf{S}(x)$

This function shows the spatial distribution of variability associated with each eigenmode. The spatial amplitude functions in the proposed model (25) are defined as (Hannchi, et al.,

2007; Marrifield & Guza, 1990; Susanto, et al., 1997; Terradas, et al., 2004; Toh, 1987; Barnett, 1983).

$$\begin{aligned} \mathbf{S}_{R(j)}(x) &= \sqrt{\boldsymbol{\Phi}_{R(j)}^H(x)\boldsymbol{\Phi}_{R(j)}(x)} \\ \mathbf{S}_{I(j)}(x) &= \sqrt{\boldsymbol{\Phi}_{I(j)}^H(x)\boldsymbol{\Phi}_{I(j)}(x)} \end{aligned} \quad (26)$$

### 3.2 Spatial phase function, $\Phi(x)$

This function shows the relative phase fluctuation among various spatial locations where  $u(x,t)$  is defined, it is given by

$$\begin{aligned} \Phi_{R(j)}(x) &= \tan^{-1} \left\{ \frac{im[\boldsymbol{\Phi}_{R(j)}(x)]}{re[\boldsymbol{\Phi}_{R(j)}(x)]} \right\} \\ \Phi_{I(j)}(x) &= \tan^{-1} \left\{ \frac{im[\boldsymbol{\Phi}_{I(j)}(x)]}{re[\boldsymbol{\Phi}_{I(j)}(x)]} \right\} \end{aligned} \quad (27)$$

### 3.3 Temporal amplitude function, $R(t)$

This function gives a measure of the temporal variability in the magnitude of the modal structure in the original field. Similar to the description of the spatial amplitude function, the temporal amplitude function is defined as

$$\begin{aligned} \mathbf{R}_{R(j)}(t) &= \sqrt{\mathbf{A}_{R(j)}^H(t)\mathbf{A}_{R(j)}(t)} \\ \mathbf{R}_{I(j)}(t) &= \sqrt{\mathbf{A}_{I(j)}^H(t)\mathbf{A}_{I(j)}(t)} \end{aligned} \quad (28)$$

### 3.4 Temporal phase function, $\theta(t)$

This function shows the temporal variation of the phase associated with the magnitude of the modal structure of  $u(x,t)$ . It is given by

$$\begin{aligned} \theta_{R(j)}(t) &= \tan^{-1} \left\{ \frac{im[\mathbf{A}_{R(j)}(t)]}{re[\mathbf{A}_{R(j)}(t)]} \right\} \\ \theta_{I(j)}(t) &= \tan^{-1} \left\{ \frac{im[\mathbf{A}_{I(j)}(t)]}{re[\mathbf{A}_{I(j)}(t)]} \right\} \end{aligned} \quad (29)$$

Equations (26-29) provide a complete characterization of any propagating effects and periodicity in the original data field which might be obscured by standard cross-spectral analysis. These equations give a measure of the space-time distribution and can be used to identify the dominant modes and their phase relationships. Furthermore, for each dominant mode of interest, a mode shape can be computed by using the spatial part of (23). This method effectively decomposes the data into spatial and temporal modes.

#### 4. Analysis of propagating features in space-time varying fields

In this section, we turn our attention to the analysis of spatial and temporal behaviour of propagating features in space-time varying fields.

##### 4.1 Space-time biorthogonal decomposition

In order to investigate travelling and standing features into a space-time varying field, the real physical field is reconstructed by taking the real part of the complex model given in (25), so, its wave form is given by (Esquivel & Messina, 2008; Esquivel, 2009)

$$\mathbf{X}(x, t) = \sum_{j=1}^p \mathbf{R}_{R(j)}(t) \mathbf{S}_{R(j)}(x) \cos(\boldsymbol{\omega}_{R(j)} t) + \sum_{j=1}^q \mathbf{R}_{I(j)}(t) \mathbf{S}_{I(j)}(x) \cos(\boldsymbol{\omega}_{I(j)} t + \mathbf{K}_{I(j)} x + \pi) \quad (30)$$

where  $\mathbf{K}(x)$  is the wave number, and  $\boldsymbol{\omega}_R(t)$ ,  $\boldsymbol{\omega}_I(t)$  represent the angular frequency of the real and imaginary wave components, respectively. The wave number is only defined for travelling waves and its components in terms of the complex representation (25) are given by:  $\mathbf{K} = d(\Phi)/dx$ , with physical units of  $rad.m^{-1}$ , and  $\boldsymbol{\omega} = d(\theta)/dt$ , in  $rad/s$ . The relationship between complex modes and the wave motion is given from average phase speeds  $c_{R(j)}$ ,  $c_{I(j)}$  obtained by using the relation  $c = \boldsymbol{\omega}/\mathbf{K}$ , in  $m/s$ .

From (30), it can be seen that the term associated with the  $j$ -th travelling wave component can be expressed as

$$\begin{aligned} \mathbf{R}_{I(j)} \mathbf{S}_{I(j)} \cos(\boldsymbol{\omega}_{I(j)} t + \mathbf{K}_{I(j)} x + \pi) &= \\ \mathbf{R}_{I(j)} \mathbf{S}_{I(j)} \{ \sin(\boldsymbol{\omega}_{I(j)} t) \sin(\mathbf{K}_{I(j)} x) - \cos(\boldsymbol{\omega}_{I(j)} t) \cos(\mathbf{K}_{I(j)} x) \} & \quad (31) \\ = -\mathbf{R}_{I(j)} \mathbf{S}_{I(j)} \cos(\boldsymbol{\omega}_{I(j)} t + \mathbf{K}_{I(j)} x) & \end{aligned}$$

where we can see that the travelling wave components are also identified as the sum of two intermodulated standing wave components with negative sign. To obtain the decomposition of the original data field in its pure standing wave components, it is necessary to compute the difference with the pure travelling wave components as

$$\mathbf{X}_{swc}(x, t) = \mathbf{X}(x, t) - \mathbf{X}_{twc}(x, t) = \sum_{j=1}^p \mathbf{R}_{R(j)}(t) \mathbf{S}_{R(j)}(x) \cos(\boldsymbol{\omega}_{R(j)} t) \quad (32)$$

with

$$\mathbf{X}_{twc}(x, t) = \sum_{j=1}^q \mathbf{R}_{I(j)}(t) \mathbf{S}_{I(j)}(x) \cos(\boldsymbol{\omega}_{I(j)} t + \mathbf{K}_{I(j)} x + \pi) \quad (33)$$

where  $\mathbf{X}_{swc}$  and  $\mathbf{X}_{twc}$  represent the decomposition of the original field given by the pure standing and travelling wave components respectively. Furthermore, the damping factor of each mode is given by its amplitude.

From the modal decomposition given in (32-33), the statistical modes are also called orthogonal temporal and spatial modes respectively. Based in the proposed model, a practical criterion for choosing the relevant modes is given in the next section.

#### 4.2 Approximation order and energy distribution in the space-time varying modes

The relationship between spatial and temporal behaviour in space-time varying fields can be obtained by noting that the spatio-temporal information can be mapped into a space and time grid, i.e., each component  $u(x,t)$  of the space-time varying field is represented by the field value at time  $t$  and spatial position  $x$ . Based on the proposed biorthogonal method, the analysis is used to determine the spatial and temporal energy distribution in the space-time varying field, a criterion for choosing the number of relevant modes from the proposed model is given by the energy percentage contained in the  $p$  and  $q$  dominant modes of the form

$$\begin{aligned} \%E(p,q) &= \frac{\sum_{j=1}^p \lambda_{(j)swc} + \sum_{j=1}^q \lambda_{(j)twc}}{\|\mathbf{X}\|_F^2} \times 100 = 99\% \\ &= \text{subject to } \operatorname{argmin}\{E(p,q) : E(p,q) \geq E_0\} \end{aligned} \quad (34)$$

where  $\|\cdot\|_F^2$  denotes the Frobenius norm,  $E_0$  is an appropriate energy level, and  $0 \leq \%E(p,q) \leq 100$  is the percentage of energy that is captured by the optimal basis. By neglecting modes corresponding to the small eigenvalues a reduced-order model can be constructed (Esquivel, 2009; Messina, et al. 2010).

We note from (34) that  $E = \|\mathbf{X}\|_F^2$ ; so the spatial-temporal energy distribution can be computed by

$$\%E_{swc} = \frac{\|\mathbf{X}_{swc}\|_F^2}{\|\mathbf{X}\|_F^2} \times 100 \quad (35)$$

which is associated with the temporal energy distribution, and

$$\%E_{twc} = \frac{\|\mathbf{X}_{twc}\|_F^2}{\|\mathbf{X}\|_F^2} \times 100 \quad (36)$$

is associated with the spatial energy distribution. Figure 2 shows a conceptual representation of spatial and temporal variability illustrating the energy distribution in a

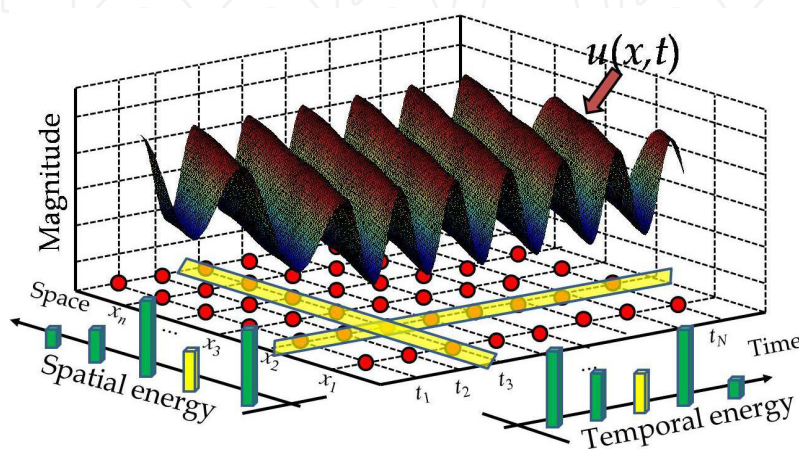


Fig. 2. Three-dimensional view of energy distribution of a time-space varying field.

space-time varying field. In an effort to better understand the mechanism of wave propagating using complex EOF analysis, in the next section is presented a first example as illustrative case to determine the theoretical fundamentals from the complex EOF analysis.

### 5. Motivating examples: Modeling of propagating wave using the covariance matrix

As illustrative case, in this section we consider a first example of wave propagation to study the modelling of propagating wave using the complex EOF analysis (Marrifield, 1990).

For simplicity, we consider a nondispersive plane wave propagating at phase speed  $c$ , and wavenumber as  $k = \omega/c$ , past an array of sensors at positions  $j$  given by

$$\mathbf{u}_j(t) = \sum_{\omega} [\alpha(\omega) \cos(kx_j - \omega t) + \beta(\omega) \sin(kx_j - \omega t)] \quad (37)$$

Expanding (37) and using identities

$$\begin{aligned} a_j(\omega) &= \alpha(\omega) \cos(kx_j) + \beta(\omega) \sin(kx_j) \\ b_j(\omega) &= \alpha(\omega) \sin(kx_j) - \beta(\omega) \cos(kx_j) \end{aligned} \quad (38)$$

we can rewritten (37) as

$$\mathbf{u}_j(t) = \sum_{\omega} \{ a_j(\omega) \cos(\omega t) + b_j(\omega) \sin(\omega t) \} \quad (39)$$

where, for this example,  $\mathbf{u}_j(t)$  is a white, band-limited signal given by

$$\alpha^2(\omega) + \beta^2(\omega) = \begin{cases} A^2, & \text{if } \omega_1 \leq \omega \leq \omega_2 \\ 0, & \text{if } \omega > \omega_2, \omega < \omega_1 \end{cases} \quad (40)$$

To obtain phase information between stations, a complex representation of (39) is invoked. Its complex covariance matrix  $\mathbf{C}_{jk} = \langle \mathbf{u}_j^*(t) \mathbf{u}_k(t) \rangle_t$ , where  $\langle \dots \rangle_t$  denotes time averaging and the asterisk complex conjugation, is given as

$$\begin{aligned} \mathbf{C}_{jk} &= \sum_{\omega} \{ [a_j(\omega) - ib_j(\omega)] e^{i\omega t} \}^* \sum_{\omega} \{ [a_k(\omega) + ib_k(\omega)] e^{-i\omega t} \} \\ &= \sum_{\omega} \{ [a_j(\omega) - ib_j(\omega)]^* [a_k(\omega) + ib_k(\omega)] \}, \\ &= \sum_{\omega} \{ [a_j(\omega) a_k(\omega) + b_j(\omega) b_k(\omega)] + i [a_j(\omega) b_k(\omega) - b_j(\omega) a_k(\omega)] \} \end{aligned} \quad (41)$$

which, simplifying and using condition given in (40),  $\mathbf{C}_{jk}$  can be rewritten as

$$\mathbf{C}_{jk} = A^2 \sum_{\omega} \{ \cos(kx_j - kx_k) - i \sin(kx_j - kx_k) \} = A^2 \sum_{\omega=\omega_1}^{\omega_2} e^{-ik(\omega) \Delta x_{jk}} \quad (42)$$

where  $\Delta x_{jk} = x_j - x_k$ . Replacing the summatory of (42) with an integral, yields

$$\mathbf{C}_{jk} = \frac{A^2}{\Delta\omega} \int_{\omega_1}^{\omega_2} e^{-ik(\omega)\Delta x_{jk}} d\omega, \quad \text{to} \quad \Delta\omega = \frac{2\pi}{T} \quad (43)$$

Integrating (43) by parts and after some algebra, we can show that

$$\mathbf{C}_{jk} = A^2 M \operatorname{sinc}\left(\frac{\Delta k \Delta x_{jk}}{2}\right) e^{-i\bar{k} \Delta x_{jk}} \quad (44)$$

with

$$\begin{aligned} \Delta k &= k(\omega_2) - k(\omega_1) \\ \bar{k} &= \frac{k(\omega_2) + k(\omega_1)}{2} \\ M &= \frac{T(\omega_2 - \omega_1)}{2\pi} \end{aligned} \quad (45)$$

where  $\Delta k$  is the wave number bandwidth,  $\Delta x$  is the array length and  $M$  is the frequency.

Equation (44) illustrates some important properties of  $\mathbf{C}$ . General algebraic expression in order to computing the eigenvalues and eigenfunctions of  $\mathbf{C}$  for an arbitrary number of sensors ( $n$ ), are very difficult to determine and which are not purposed here. For the case of two sensors, the above model can be reduced to

$$\mathbf{C}_{jk} = \begin{bmatrix} A^2 M & A^2 M \operatorname{sinc}\left(\frac{\Delta k(x_1 - x_2)}{2}\right) e^{-i\bar{k}(x_1 - x_2)} \\ A^2 M \operatorname{sinc}\left(\frac{\Delta k(x_2 - x_1)}{2}\right) e^{-i\bar{k}(x_2 - x_1)} & A^2 M \end{bmatrix}, \quad j, k = 1, 2 \quad (46)$$

From the relation above is followed that the eigenvalues of  $\mathbf{C}$  are given by  $\det[\lambda \mathbf{I} - \mathbf{C}_{j,k}]$ , i.e., it is easy to see further that

$$\lambda_{1,2} = A^2 M \pm A^2 M \left| \operatorname{sinc}\left(\frac{\Delta k \Delta x}{2}\right) \right| = A^2 M \left[ 1 \pm \left| \operatorname{sinc}\left(\frac{\Delta k \Delta x}{2}\right) \right| \right] \quad (47)$$

It then follows that the eigenvectors of  $\mathbf{C}$  defined as  $[\lambda \mathbf{I} - \mathbf{C}_{j,k}] \mathbf{B} = 0$ , are given by

$$\begin{bmatrix} A^2 M \operatorname{sinc}\left(\frac{\Delta k \Delta x}{2}\right) & -A^2 M \operatorname{sinc}\left(\frac{\Delta k \Delta x}{2}\right) e^{-i\bar{k} \Delta x} \\ -A^2 M \operatorname{sinc}\left(\frac{\Delta k \Delta x}{2}\right) e^{i\bar{k} \Delta x} & A^2 M \operatorname{sinc}\left(\frac{\Delta k \Delta x}{2}\right) \end{bmatrix} \begin{bmatrix} B_{1,1} \\ B_{2,1} \end{bmatrix} = \begin{bmatrix} 0 \\ 0 \end{bmatrix} \quad (48)$$

and

$$\begin{bmatrix} -A^2 M \operatorname{sinc}\left(\frac{\Delta k \Delta x}{2}\right) & -A^2 M \operatorname{sinc}\left(\frac{\Delta k \Delta x}{2}\right) e^{-i\bar{k} \Delta x} \\ -A^2 M \operatorname{sinc}\left(\frac{\Delta k \Delta x}{2}\right) e^{i\bar{k} \Delta x} & -A^2 M \operatorname{sinc}\left(\frac{\Delta k \Delta x}{2}\right) \end{bmatrix} \begin{bmatrix} B_{1,2} \\ B_{2,2} \end{bmatrix} = \begin{bmatrix} 0 \\ 0 \end{bmatrix} \quad (49)$$

which can be simplified to

$$\begin{bmatrix} 1 & -e^{-i\bar{k} \Delta x} \\ 0 & 0 \end{bmatrix} \begin{bmatrix} B_{1,1} \\ B_{2,1} \end{bmatrix} = \begin{bmatrix} 0 \\ 0 \end{bmatrix} \quad \text{and,} \quad \begin{bmatrix} 1 & e^{-i\bar{k} \Delta x} \\ 0 & 0 \end{bmatrix} \begin{bmatrix} B_{1,2} \\ B_{2,2} \end{bmatrix} = \begin{bmatrix} 0 \\ 0 \end{bmatrix} \quad (50)$$

where

$$B_{1,1} = B_{2,1} e^{-i\bar{k} \Delta x}, \quad \text{if } B_{2,1} = T, \quad B_{1,1} = T e^{-i\bar{k} \Delta x}$$

$$\begin{bmatrix} B_{1,1} \\ B_{2,1} \end{bmatrix} = \begin{bmatrix} e^{-i\bar{k} x_1} \\ e^{-i\bar{k} x_2} \end{bmatrix} T, \quad \text{with } T = e^{-i\bar{k} x_2} \quad (51)$$

and

$$B_{1,2} = -B_{2,2} e^{-i\bar{k} \Delta x}, \quad \text{if } B_{2,2} = -T, \quad B_{1,2} = T e^{-i\bar{k} \Delta x}$$

$$\begin{bmatrix} B_{1,2} \\ B_{2,2} \end{bmatrix} = \begin{bmatrix} e^{-i\bar{k} x_1} \\ -e^{-i\bar{k} x_2} \end{bmatrix} T, \quad \text{with } T = e^{-i\bar{k} x_2} \quad (52)$$

The following observations can be made from the analysis:

1. As can be seen from (51) and (52), the method yields complex conjugate eigenvectors and an average wave number,  $\bar{k}$ .
2. The value  $\bar{k} x_j$  gives the mode shape; this can be used for detection of wave propagating into original field and can be useful to identify the dominant stations involved in the propagating wave of dynamical oscillations. We remark that the performance of the complex EOF analysis as measured by the percentage of variance given in (47) depends on the spread in wave number relative to the array size, as the parameter  $\Delta k \Delta x$  decreases, more of the variance is contained in the lowest complex EOF modes.
3. A point of particular interest is that, as a standard technique for describing coherent variability in spatial data, a relatively wide number bandwidth [ $\Delta k \Delta x > 0(2\pi)$ ] results from (47).

The development given in this section indicates that modal spatial patterns from a time domain complex EOF analysis may be computed in a straightforward manner. In the next section, data obtained from GPS-based multiple phasor measurements units from a real event of seismic wave of an earthquake are used to study the practical applicability of the method to characterize spatio-temporal behaviour in wide-area systems. Additionally, we discuss the practical computation of mode shape identification in relation to the proposed decomposition from measurements data that can be used to identify coherence groups in vast wide-area interconnected systems where the propagating wave are given.

## 6. Complex EOF analysis to wide-area system oscillatory dynamics

This section examines the application of the proposed technique to assess oscillations patterns in dynamical systems. Attention is focused on the identification of critical modes and the associated areas involved in the oscillations. In order to test the ability of the method to analyze complex oscillations, we use data recorded from time-synchronized measurements. The data were obtained from the Geophysical Institute of the National Autonomous University of México. A brief description of the data is given below.

At local time 15:36:14.730, October 9, 1995 a submarine earthquake was occurred near the Mexican coast (Colima-Jalisco); this earthquake was recorded by sixteen stations of phasor measurement units (PMUs) over a 225 s window sampled with time interval of 0.005 s during its propagating that was felt over much of Jalisco and parts of Colima. We examined evidence of seismic wave arrival times of the earthquake in PMUs based in global positioning system (GPS). For simplicity, in Table 1 is given the description of the locations of each station. This earthquake was located at a depth of 5km about (18.740°N, 104.670°W). Figure 3 shows with a geographical diagram the PMUs locations and the location of the event.

PMUs	Station	Location		
		Latitude N	Longitude W	Altitude (msnm)
1	Ciudad Guzman	19.6°	103.4°	1507
2	Santa Rosa corona centro	20.912°	103.708°	770
3	Santa Rosa margen izquierda	20.912°	103.708°	780
4	Ciudad Granja	20.672°	103.398°	1680
5	Jardines del sur	20.648°	103.366°	1583
6	Arcos	20.671°	103.362°	1585
7	Obras publicas Zapopan	20.699°	103.361°	1561
8	Miravalle	20.633°	103.342°	1610
9	Rotonda	20.673°	103.34°	1542
10	San Rafael	20.654°	103.311°	1560
11	Planetario	20.717°	103.308°	1543
12	Tonala	20.641°	103.279°	1660
13	CICEJ superficie	20.6°	103.2°	1575
14	CICEJ pozo 9m	20.6°	103.2°	1566
15	CICEJ pozo 35m	20.6°	103.2°	1540
16	Oblatos	20.6°	103.2°	1580
	Earthquake	18.740°	104.670°	5km (depth)

Table 1. Description and location of stations of phasor measurements units.

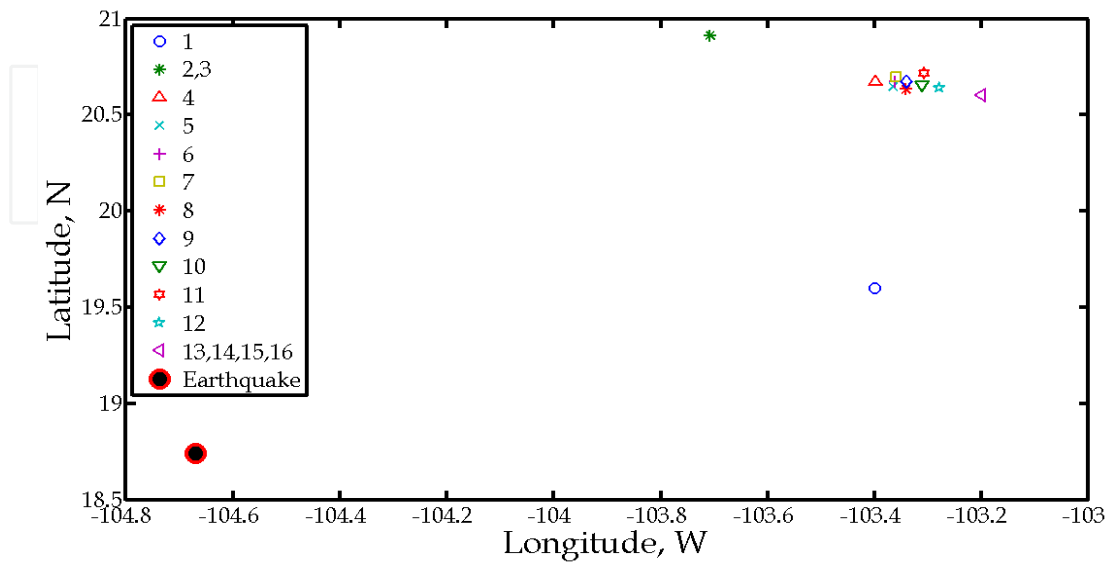


Fig. 3. Schematic showing the location of stations of the PMUs.

During the time interval 15:36:14.730-15:40:42 the earthquake experiment severe fluctuations where its seismic wave components such as frequency and amplitude were felt. Figures 4,5 and 6 give an extraction from PMUs measurements of this event showing the observed oscillations in the selected stations, where for simplicity, the seismic wave features are selected in longitude, latitude and altitude components. As a first step towards the development of the proposed methodology, the observed records are placed in a data matrix representing equally spaced measurements in sixteen different geographical locations. For our simulation, 45000 snapshots are available. Each time series is then augmented with an imaginary component by the Hilbert analysis to provide phase information and the corresponding biorthogonal decomposition is applied to the dataset. System measurements in Figs. 4,5 and 6 demonstrate significant variability suggesting a nonstationary process in both space and time. Furthermore, in these figures are shown the associated mode to the travelling wave components based in the proposed method of biorthogonal decomposition. The results clearly show the seismic wave decomposition, it is evident that the travelling wave mode in longitude and latitude is quite prominent at CICEJ and Oblatos stations, while that in the Ciudad Guzman and Santa Rosa stations are more stronger in altitude. A point of particular interest is the agreement between the results from the proposed model and the real behaviour of the space-time variability presented during the seismic wave. In (Ortiz, et al., 1998) was analyzed the tsunami data generated by the Colima-Jalisco earthquake, where the results of the tsunami arrival time are consistent with the presented in this analysis.

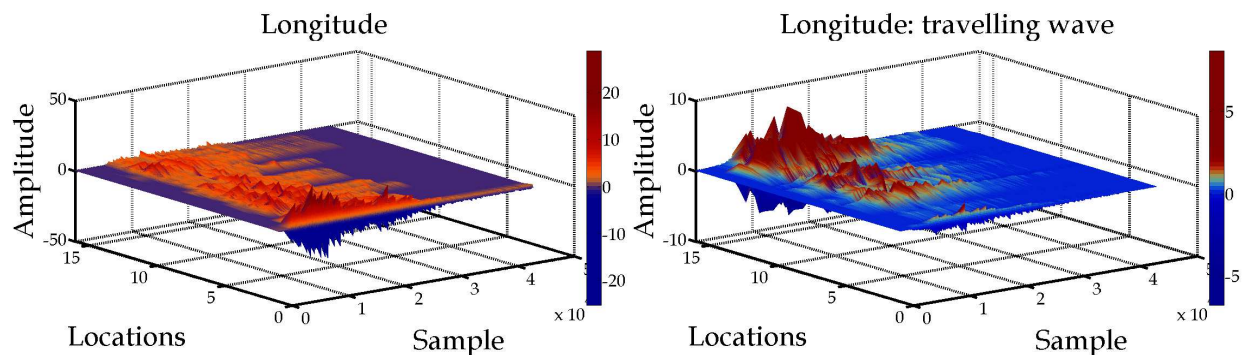


Fig. 4. Seismic fluctuating components in longitude and the leading mode showing spatio-temporal variability in the location of stations.

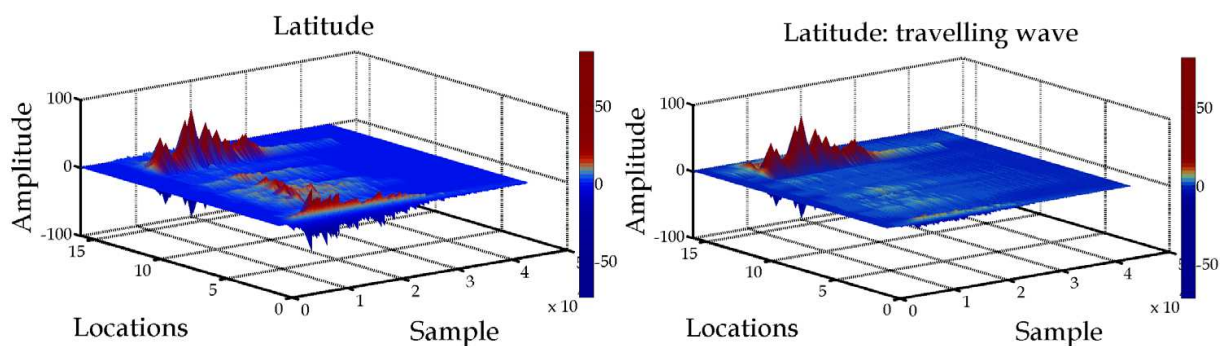


Fig. 5. Seismic fluctuating components in latitude and the leading mode showing spatio-temporal variability in the location of stations.

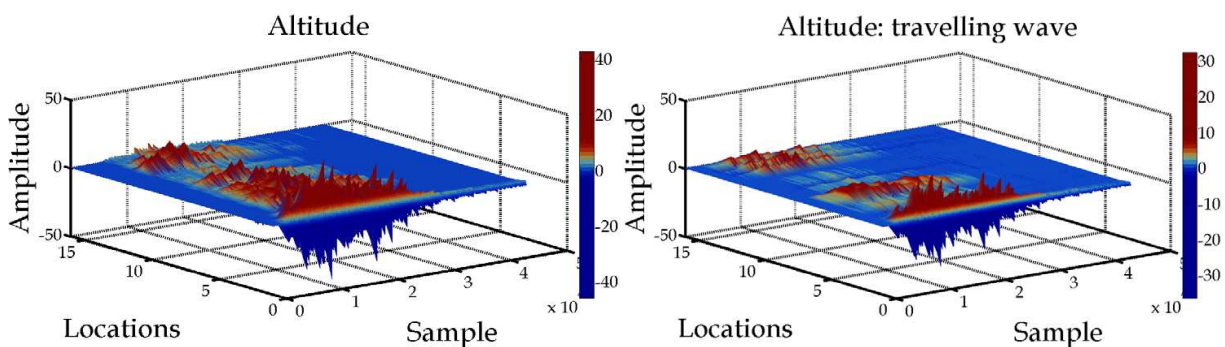


Fig. 6. Seismic fluctuating components in altitude and the leading mode showing spatio-temporal variability in the location of stations.

Additional insight into the frequency variability of the seismic oscillations can be obtained from the analysis of instantaneous frequency. Recognizing that the instantaneous frequency is the derivative of the temporal phase function given from the proposed model (30), the instantaneous frequency is estimated for each mode of concern. However, other approach can be used to characterize the spectral behaviour that requires other analytical formulations (Ortiz, et al., 2000).

The study focuses on the travelling wave mode which is the mode that captures most of the variability in the seismic wave. Figure 7 gives the spectrogram of the travelling wave modes associated to the longitude, latitude and altitude for the interval of interest in this study.

From this figure is evident that the earthquake was feeling with fluctuating components after 10 s since it was occurred.

Spectral analysis results for the leading travelling wave shows that the main power is concentrated in oscillations with frequencies about 4.8, 5.2 and 4.0 Hz, to the longitude, latitude and altitude components which are associated with the major time interval of the seismic wave.

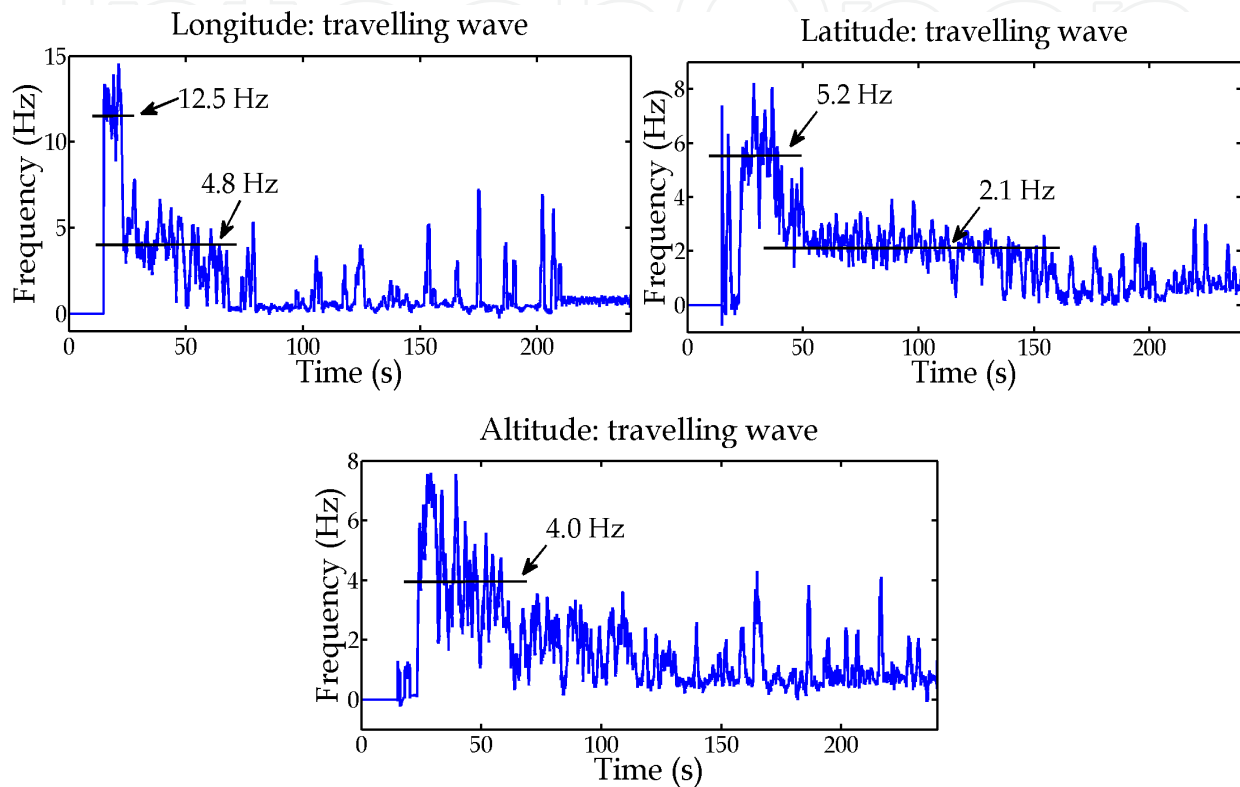


Fig. 7. Spectrograms to the seismic wave from the longitude, latitude and altitude components using the travelling wave modes.

One of the most attractive features of the proposed technique is its ability to detect changes in the mode shape properties of critical modes arising from systems. Changes in the mode shape may indicate changes in topology of the dynamic systems and may be useful for the design of special protection systems. This is a problem that has been recently addressed using spectral correlation analysis (Wallaschek, 1988).

Using the spatial phase and amplitude (the mode shape), the phase relationship between key system locations can be determined. In this analysis, we display the complex values as a vector with the length of its arrow proportional to eigenvector magnitude and direction equal to the eigenvector phase. Figure 8 shows the mode shape for the three travelling wave computed from the longitude, latitude and altitude components for the seismic wave, this information is useful to identify the dominant stations involved in the oscillations. Simulation results to the mode shape clearly show that the CICEJ (13,14,15) stations are more stronger evident at the longitude components; CICEJ (13,14) stations in latitude, and finally the Ciudad Guzman, Los Arcos, CICEJ (1,6,13,14) stations in altitude.

These results are in general agreement with the shown in Figs. 4,5 and 6 from the observed oscillations giving validity to the results. The new results provide clarification on the exact phase relationship between key stations as a function of space.

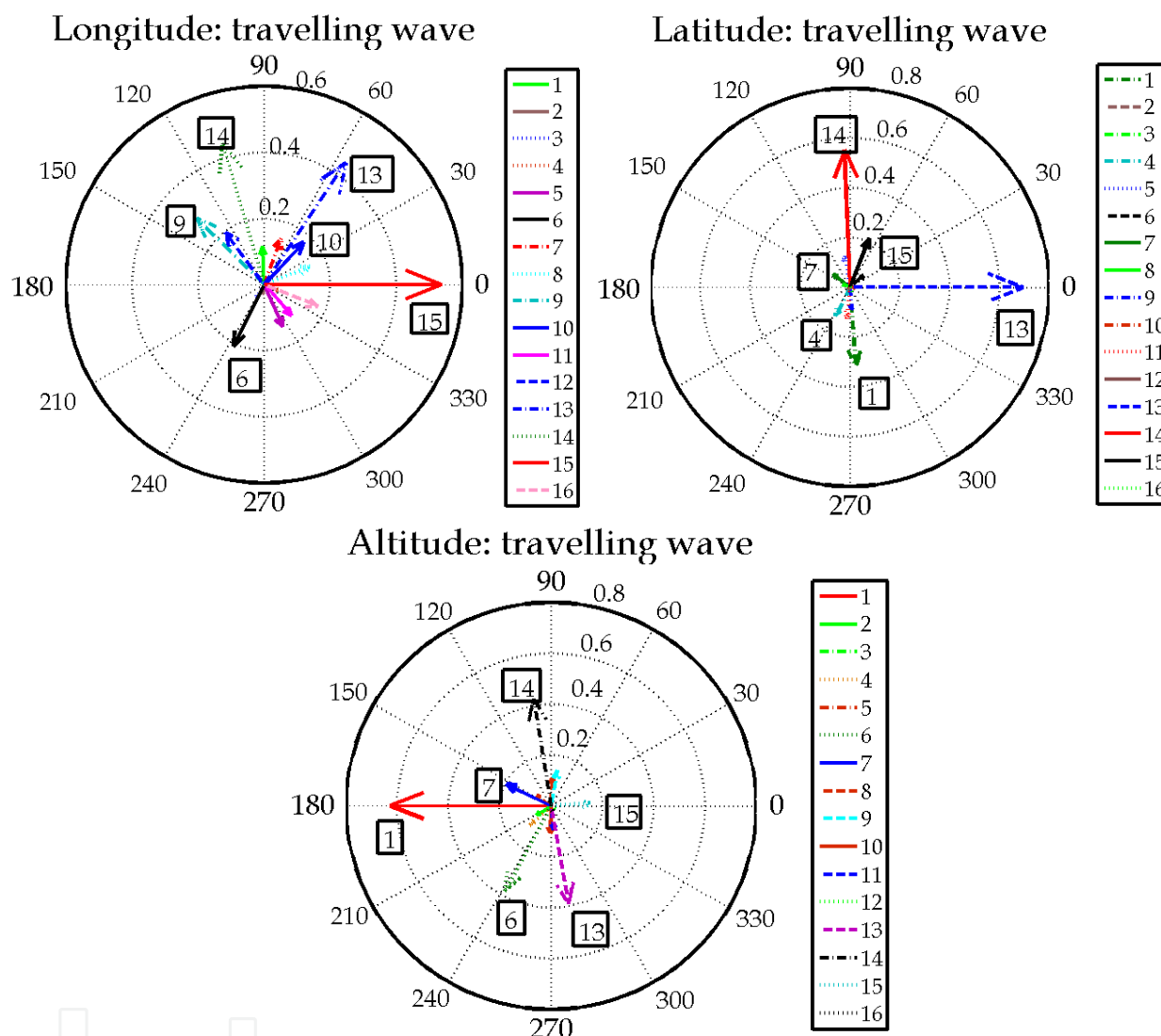


Fig. 8. Mode shape fluctuating in longitude, latitude and amplitude of the leading mode showing the phase relationship between stations.

## 7. Conclusion

Approaches for detection of propagation features in space-time varying system measurements through its travelling and standing components are proposed.

The conceptual framework developed provides bases for the analysis, detection, and simplification of seismic wave components through use of wide-area monitoring schemes such as global positioning systems (GPS) based in multiple phasor measurements units (PMUs) for interconnected systems, and enables the simultaneous study of synchronized measurements. The main advantage of the approach is its ability to compress the variability of large data sets into the fewest possible number of spatial and temporal modes. The

technique is especially attractive, because, it does not require previous notion about the behaviour associated with abrupt changes in system topology or operating conditions.

Complex empirical orthogonal function analysis is shown to be a useful method to identify standing and travelling patterns in wide-area system measurements. In the use of information in interconnected systems, spatio-temporal analysis of wide-area time-synchronized measurements shows that transient oscillations may manifest highly complex phenomena, including nonstationary behaviour. Numerical results show that the proposed method can provide accurate estimation of nonstationary effects, modal frequency, mode shapes, and time instants of intermittent transient responses. This information is important to determine strategies for wide-area monitoring and special protection systems.

The main contributions in this chapter are based in the estimation of propagating and standing features in space-time varying processes using statistical techniques to identify oscillatory activity in interconnected systems through the use of wide-area monitoring schemes in interconnected systems.

The proposed technique is based on the complex correlation structure from space-time varying fields, which can treat both, spatial and temporal information; this provides a global picture on the system behaviour to characterize oscillatory dynamics. Its significant drawbacks are associated to treat with their space-time scales. These include geographical distribution and the time interval to the modal extraction using measured data. For some applications may be desirable to have these data at very high space-time resolution that allow the study of processes close to inertial frequency, then a technique of space-time interpolation can be used. Wide-area monitoring may prove invaluable in interconnected system dynamic studies by giving a quick assessment of the damping and frequency content of dominant system modes after a critical contingency. The alternative technique based on space-time dependent complex EOF analysis of measured data is proposed to resolve the localized nature of transient processes and to extract dominant temporal and spatial information.

## 8. Acknowledgment

This work was supported under a scholarship granted by CONACYT México no. 172551 to CINVESTAV Guadalajara. We thank to the Geophysical Institute of the National Autonomous University of México for their support and facility to use the data presented in this work.

## 9. References

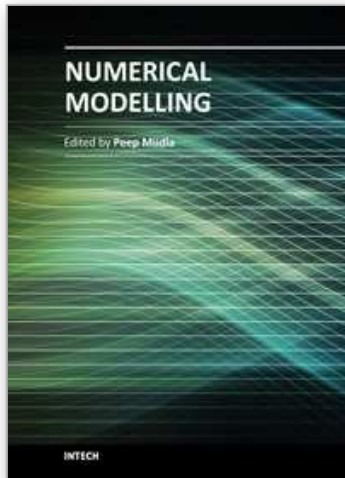
- Achatz, U.; Schmitz, G. & Greisiger, K.-M. (1995). Principal Interaction Patterns in Baroclinic Wave Life Cycles, *Journal of the Atmospheric Sciences*, Vol.52, No.18, (September 1995), pp. 3201-3213, ISSN 15200469
- Aubry, N.; Guyonnet, R. & Lima, R. (1990). Spatiotemporal Analysis of Complex Signals: Theory and Applications, *Journal of Statistical Physics*, Vol.64, No.3-4, (January 1991), pp. 683-738, ISSN 00224715

- Barnett, T. P. (1983). Interaction of the Monsoon and Pacific Trade Wind Systems at Interannual Time Scales. Part I: The Equatorial Zone, *Monthly Weather Review*, Vol.111, No.4, (April 1983), pp. 756-773, ISSN 15200493
- Dankowicz, H.; Holmes, P.; Berkooz, G. & Elezgaray, J. (1996). Local Models of Spatio-Temporally Complex Fields, *Physica D*, Vol.90, No.1996, (August 1995), pp. 387-407, ISSN 01672789
- DelSole, T. (2001). Optimally Persistent Patterns in Time-Varying Fields, *Journal of Atmospheric Sciences*, Vol.58, No.11, (June 2001), pp. 1341-1356, ISSN 207053106
- Esquivel, P. (2009). Wide-Area Wave Motion Analysis Using Complex Empirical Orthogonal Functions, *International Conference on Electrical Engineering, Computing Science and Automatic Control (ICEEE)*, ISBN 978-1-4244-4688-9, Toluca, Estado de México, México, November 10-13, 2009
- Esquivel, P.; Barocio, E.; Andrade, M. A. & Lezama, F. (2009). Complex Empirical Orthogonal Function Analysis of Power-System Oscillatory Dynamics, In: *Inter-area Oscillations in Power Systems: A Nonlinear and Nonstationary Perspective*, A. R. Messina, Springer, 159-187, ISBN 9780387895291, New York, United States
- Esquivel, P. & Messina, A. R. (2008). Complex Empirical Orthogonal Function Analysis of Wide-Area System Dynamics, *IEEE Power and Energy Society General Meeting Scheduled (PES)*, ISBN 978-1-4244-1905-0, Pittsburgh, Pennsylvania, United States, July 20-24, 2008
- Feeny, B. F. (2008). A Complex Orthogonal Decomposition for Wave Motion Analysis, *Journal of Sound and Vibration*, Vol.310, No.1-2, (November 2008), pp. 77-90, ISSN 0022460X
- Feeny, B. F. & Kappagantu, R. (1998). On the Physical Interpretation of Proper Orthogonal Modes in Vibrations, *Journal of Sound and Vibration*, Vol.211, No.4, (Abril 1999), pp. 607-616, ISSN 0022460X
- Fuentes, M. (2006). Testing for Separability of Spatial-Temporal Covariance Functions, *Journal of Statistical Planning and Inference*, Vol.136, No.2, (July 2004), pp. 447-466, ISSN 03783758
- Han, S. & Feeny B. F. (2003). Application of Proper Orthogonal Decomposition to Structural Vibration Analysis, *Mechanical Systems and Signals Processing*, Vol.17, No.5, (September 2003), pp. 989-1001, ISSN 08883270
- Hannachi, A.; Jolliffe, I. T. & Stephenson, D. B. (2007). Empirical Orthogonal Functions and Related Techniques in Atmospheric Science: A Review, *International Journal of Climatology*, Vol.27, No.9, (July 2007), pp. 1119-1152, ISSN 08998418
- Horel, J. D. (1984). Complex Principal Component Analysis: Theory and Examples, *Journal of Climate and Applied Meteorology*, Vol.23, No.12, (September 1984), pp. 1660-1673, ISSN 07333021
- Hasselmann, K. (1988). PIP and POPs: the Reduction of Complex Dynamical Systems Using Principal Interaction and Oscillation Patterns, *Journal of Geophysical Research*, Vol.93, No.D9, (September 1988), pp. 11015-11021, ISSN 01480227
- Holmes, P.; Lumley, J. L. & Berkooz, G. (1996). *Turbulence, Coherent Structures, Dynamical Systems and Symmetry*, Cambridge University Press, ISBN 0521634199, New York, United States

- Hostelling, H. (1933). Analysis of a Complex of Statistical Variables into Principal Components, *Journal of Educational Psychology*, Vol.24, No.6, (September 1933), pp. 417-441, ISSN 19392176
- Kaihatu, J. M.; Handler, R. A.; Marmorino, G. O. & Shay, L. K. (1997). Empirical Orthogonal Function Analysis of Ocean Surface Currents Using Complex and Real-Vector Methods, *Journal of Atmospheric and Oceanic Technology*, Vol.15, No.1, (September 1997), pp. 927-941, ISSN 395295004
- Kosambi, D. D. (1943). Statistics in Function Space, *Journal of Indian Mathematical Society*, Vol.7, No.46, (June 1943) pp. 76-88, ISSN 00195839
- Kwasniok, F. (1996). The reduction of Complex Dynamical Systems Using Principal Interaction Patterns, *Physica D: Nonlinear Phenomena*, Vol.92, No.1-2, (April 1996), pp. 28-60, ISSN 01672789
- Kwasniok, F. (2007). Reduced Atmospheric Models Using Dynamically Motivated Basis Functions, *Journal of the Atmospheric Sciences*, Vol.64, No.10, (October 2007), pp. 3452-3474, ISSN 00224928
- Marrifield, M. A. & Guza, R. T. (1990). Detecting Propagating Signals with Complex Empirical Orthogonal Functions: A Cautionary Note, *Journal of Physical Oceanography*, Vol.20, No.10, (February 1990), pp. 1628-1633, ISSN 15200485
- Messina, A. R.; Esquivel, P. & Lezama, F. (2010). Time-Dependent Statistical Analysis of Wide-Area Time-Synchronized Data, *Journal of Mathematical Problems in Engineering (MPE)*, Vol.2010, No.2010, (Abril 2010), pp. 1-17, ISSN 1024123X
- Messina, A. R.; Esquivel, P. & Lezama, F. (2011). Wide-Area PMU Data Monitoring Using Spatio-Temporal Statistical Models, *2011 IEEE/PES Power Systems Conferences and Exposition*, ISBN 978-1-61284-789-4, Phoenix, Arizona, United States, March 20-23, 2011
- Leonardi, A. P.; Morey, L. S. & O'Brien, J. J. (2002). Interannual Variability in the Eastern Subtropical North Pacific Ocean, *Journal of Physical Oceanography*, Vol.32, No.1, (June 2002), pp. 1824-1837, ISSN 15200485
- Lezama, F.; Rios, A. L.; Esquivel, P. & Messina, A. R. (2009). A Hilbert-Huang Based Approach for On-Line Extraction of Modal Behavior from PMU Data, *IEEE PES 41st North American Power Symposium (NAPS)*, ISBN 978-1-4244-4428-1, Starkville, Mississippi, United States, October 4-6, 2009
- Oey, L.-Y. (2007). Loop Current and Deep Eddies, *Journal of Physical Oceanography*, Vol.38, No.1, (October 2007), pp. 1426-1449, ISSN 11753818
- Ortiz, M.; Gomez-Reyes, E. & Velez-Muñoz, S. (2000). A Fast Preliminary Estimation Model for Transoceanic Tsunami Propagation, *Geophysical International*, Vol.39, No.3, (June 2000), pp. 207-220, ISSN 00167169
- Ortiz, M.; Singh, S. K.; Pacheco, J. & Kostoglodov, V. (1998). Rupture Length of the October 9, 1995 Colima-Jalisco Earthquake ( $M_w$ ) Estimated from Tsunami Data, *Geophysical Research Letters*, Vol.25, No.15, (August 1998), pp. 2857-2860, ISSN 00948534
- Spletzer, M.; Raman, A. & Reifenberger, R. (2010). Spatio-Temporal Dynamics of Microcantilevers Tapping on Samples Observed Under an Atomic Force Microscope Integrated with a Scanning Laser Doppler Vibrometer: Applications to Proper Orthogonal Decomposition and Model Reduction, *Journal of Micromechanics and Microengineering*, Vol.20, No.8, (August 2010), pp. 1088-1098, ISSN 09601317

- Susanto, R. D.; Zheng, Q. & Yan, X. H. (1997). Complex Singular Value Decomposition Analysis of Equatorial Waves in the Pacific Observed by TOPEX/Poseidon Altimeter, *Journal of Atmospheric and Oceanic Technology*, Vol. 15, No.1, (July 1997), pp. 764-774, ISSN 197163501
- Terradas, J.; Oliver, R. & Ballester, J. L. (2004). Application of Statistical Techniques to the Analysis of Solar Coronal Oscillations, *The Astrophysical Journal*, Vol.614, No.1, (October 2004), pp. 435-447, ISSN 0004637X
- Toh, S. (1987). Statistical Model with Localized Structures Describing the Spatial-Temporal Chaos of Kuramoto-Sivashinky Equation, *Journal of the Physical Society of Japan*, Vol.56, No.3, (March 1987), pp. 949-962, ISSN 00319015
- Wallaschek, J. (1988). Integral Covariance Analysis for Random Vibrations of Linear Continuous Mechanical Systems, *Dynamical and Stability of Systems*, Vol.3, No.1-2, (January 1988), pp. 99-107, ISSN 14565390

IntechOpen



## **Numerical Modelling**

Edited by Dr. Peep Miidla

ISBN 978-953-51-0219-9

Hard cover, 398 pages

**Publisher** InTech

**Published online** 23, March, 2012

**Published in print edition** March, 2012

This book demonstrates applications and case studies performed by experts for professionals and students in the field of technology, engineering, materials, decision making management and other industries in which mathematical modelling plays a role. Each chapter discusses an example and these are ranging from well-known standards to novelty applications. Models are developed and analysed in details, authors carefully consider the procedure for constructing a mathematical replacement of phenomenon under consideration. For most of the cases this leads to the partial differential equations, for the solution of which numerical methods are necessary to use. The term Model is mainly understood as an ensemble of equations which describe the variables and interrelations of a physical system or process. Developments in computer technology and related software have provided numerous tools of increasing power for specialists in mathematical modelling. One finds a variety of these used to obtain the numerical results of the book.

### **How to reference**

In order to correctly reference this scholarly work, feel free to copy and paste the following:

P. Esquivel, D. Cabuto, V. Sanchez and F. Chan (2012). Biorthogonal Decomposition for Wide-Area Wave Motion Monitoring Using Statistical Models, Numerical Modelling, Dr. Peep Miidla (Ed.), ISBN: 978-953-51-0219-9, InTech, Available from: <http://www.intechopen.com/books/numerical-modelling/biorthogonal-decomposition-for-wide-area-wave-motion-monitoring-using-statistical-models>

**INTECH**  
open science | open minds

### **InTech Europe**

University Campus STeP Ri  
Slavka Krautzeka 83/A  
51000 Rijeka, Croatia  
Phone: +385 (51) 770 447  
Fax: +385 (51) 686 166  
[www.intechopen.com](http://www.intechopen.com)

### **InTech China**

Unit 405, Office Block, Hotel Equatorial Shanghai  
No.65, Yan An Road (West), Shanghai, 200040, China  
中国上海市延安西路65号上海国际贵都大饭店办公楼405单元  
Phone: +86-21-62489820  
Fax: +86-21-62489821

© 2012 The Author(s). Licensee IntechOpen. This is an open access article distributed under the terms of the [Creative Commons Attribution 3.0 License](#), which permits unrestricted use, distribution, and reproduction in any medium, provided the original work is properly cited.

IntechOpen

IntechOpen